

Light to investigate (read) and operate (write) molecular devices and machines

Q1 Q2

Cite this: DOI: 10.1039/c3cs60400d

Paola Ceroni, Alberto Credi and Margherita Venturi

Q3

The development of multicomponent (supramolecular) systems that can perform predetermined functions under external control – *i.e.*, molecular devices – is a challenging task in chemistry and a fascinating objective in the frame of a bottom-up approach to nanostructures. In this context light signals can be conveniently used both for supplying energy to the system and for probing its states and transformations. The aim of this tutorial review is to recall a few basic aspects of light-induced processes that can be used to “write” and “read” onto molecular and supramolecular systems. These principles are illustrated through some examples of artificial molecular devices and machines taken from our work, which provide a flavour of current research. They are molecular and supramolecular systems that operate and/or perform valuable functions by exploiting photoinduced energy- or electron-transfer processes, photoisomerization reactions, or photoinduced proton transfer. The choice of these examples was based on both their intrinsic importance for the referred topic and their educational value. In the last section of the review potential applications, limitations and future directions of the research in the field of artificial molecular devices and machines are also discussed.

Received 5th November 2013

DOI: 10.1039/c3cs60400d

www.rsc.org/csr

Key learning points

- (a) Excited state deactivations in molecular and supramolecular systems
- (b) Light as reading and writing inputs on a molecular device
- (c) Key factors to obtain an efficient molecular light-harvesting antenna
- (c) Photoinduced electron transfer to operate molecular machines
- (d) Light induced isomerization reactions to control metal ion coordination, obtain memory effects, and switch luminescence signals in supramolecular systems

1. Introduction

The interaction between light and matter lies at the heart of most important processes of life.¹ Photons are exploited by natural systems as both quanta of energy and elements of information. Light constitutes an energy source and is consumed (or, more precisely, converted) in large amounts in the natural photosynthetic process, while it plays the role of a signal in vision-related processes, where the energy used to run the operation is biologic in nature. A variety of functions can also be obtained from the interaction between light and matter in artificial systems. The type and utility of such functions depend on the degree of complexity and organization of the chemical systems that receive and process the photons.

Supramolecular chemistry, an intensively grown area of chemistry during the past three decades, deals with the “organised entities of higher complexity that result from the association of two or more chemical species held together by intermolecular forces”² and is intimately related to biological systems and processes. Owing to the progress of synthetic chemistry, it has become possible to design and synthesize supramolecular systems composed of a remarkable number of molecular components capable of self-assembling under appropriate experimental conditions. Chemical systems can also be constructed where distinct molecular components are held together by coordination and covalent bonds (as in grids, racks, arrays or dendrimers) or even mechanically linked to each other (as in catenanes and rotaxanes). According to the above definition, such systems would not belong to the supramolecular realm; it was pointed out, however, that species that are not strictly supramolecular under the viewpoints of chemical bonds can exhibit, in fact, supramolecular behaviour as far as their physico-chemical properties (and the related emerging functions) are concerned.³

Q4 Dipartimento di Chimica “Giacomo Ciamician” and Interuniversity Center for the Chemical Conversion of Solar Energy (SolarChem), Alma Mater Studiorum – Università di Bologna, via Selmi 2, 40126 Bologna, Italy

All these species have their multicomponent nature in common, *i.e.*, the fact that they are made by a discrete number of molecular units linked together by a variety of forces, from weak electrostatic interactions to covalent bonds.

In the frame of research on supramolecular chemistry, the idea began to arise^{2,4,5} that the concept of a macroscopic device and machine can be transferred to the molecular level. In short, a molecular device can be defined⁶ as an assembly of a discrete number of molecular components designed to perform a function under appropriate external stimulation. A molecular machine^{6–8} is a particular type of device where the function is achieved through the mechanical movements of its molecular components.

Much of the inspiration to construct molecular devices and machines comes from the outstanding progress of molecular biology that has begun to reveal the secrets of natural nanomachines which constitute the material base of life. Surely, the supramolecular architectures of the biological world are themselves the premier, proven examples of the feasibility and utility of nanotechnology, and constitute a sound rationale for attempting the realization of artificial molecular devices. The bottom-up construction of devices and machines as complex as those present in nature is a prohibitive task. Therefore, chemists have tried (i) to construct much simpler systems, without mimicking the complexity of biological structures, (ii) to understand the principles and processes at the basis of their operation, and (iii) to investigate the challenging problems posed by interfacing these systems with the macroscopic world, particularly as far as energy supply and information exchange are concerned.

In analogy to their macroscopic counterparts, molecular devices and machines need energy to operate and signal to

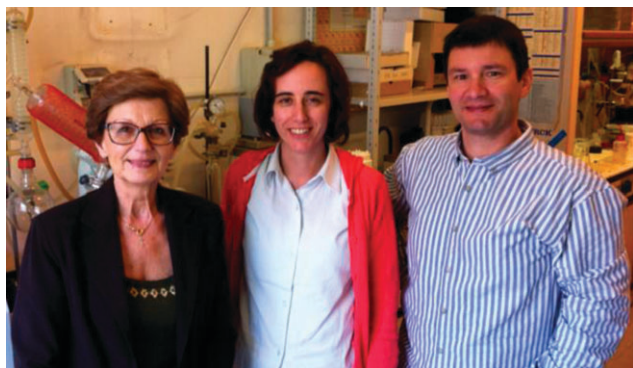
communicate with the operator. Light provides an answer to this dual requirement.⁹ Indeed, photons can trigger a photoreaction that causes (“writes”) some structural and/or electronic changes in the species, which are reflected in the modification of its properties. Light can also be useful to “read” the state of the system, and thus to control and monitor its operation, because the interactions between the components of the device often affect the photonic response of the system.

The aim of this tutorial review is to recall a few basic aspects of light-induced processes that can be exploited to “write” and “read” onto molecular and supramolecular systems. These principles will be illustrated through some selected examples taken from our work, which are also intended to provide a flavour of current research. The choice of the examples was based not only on the intrinsic interest of the topic itself or its possible applications, but also on its educational value. Finally, we shall discuss potential applications, limitations and future directions.

2. From molecular to supramolecular photochemistry

At the molecular level, absorption of light (in the range 200–1000 nm) yields electronically excited states, which are metastable species with different chemical properties compared to the ground-state molecules and which undergo rapid deactivation by competitive processes: (i) radiative (rate constant, k_r) and (ii) non-radiative processes (k_{nr}), and (iii) photoreactions (k_p).

When dealing with a supramolecular system, *e.g.* a triad A–L–B constituted by two chromophores A and B linked by a



Paola Ceroni (center), Alberto Credi (right) and Margherita Venturi (left)

promoted to associate professor in 2005. His research is focused on the design and investigation of photo- and electro-active molecules, supramolecular systems, and nanoparticles with the purpose of developing nanoscale devices and machines. He has received several scientific awards and is co-author of more than 200 scientific papers ($h = 51$), reviews and book chapters, two monographs, and a handbook of photochemistry.

Margherita Venturi (left) received her degree in Chemistry (1971) from the University of Bologna. In 1992 she became associate professor and in 2005 was promoted to full professor. From 1972 to 1991 she worked at the National Research Council of Bologna where she mainly studied, by means of pulsed and continuous radiolytic techniques, the electron-transfer processes involved in model systems for the conversion of solar energy. Her present research activity is focused on the design and investigation of photo- and electro-active supramolecular systems that behave as molecular devices and machines. She is co-author of more than 200 scientific papers ($h = 50$), including reviews, book chapters, and two monographs.

Paola Ceroni (center) is an associate professor at the University of Bologna. In 1998 she obtained her PhD, which won the Semerano prize from the Italian Chemical Society, at the University of Bologna, after a period in the United States (Prof. Allen J. Bard's laboratory). Her current research is focused on the photochemistry and electrochemistry of supramolecular systems with particular emphasis towards photoactive dendrimers, which has recently been funded by an ERC Starting Grant. She is co-author of more than 130 scientific papers in international refereed journals ($h = 33$), including reviews, book chapters, and one monograph.

Alberto Credi (right) received his degree in Chemistry from the University of Bologna where, after a research period in the United States, he also earned his PhD in Chemical Sciences. In 1999 he became assistant professor of Chemistry at his Alma Mater, and was

bridge L, light absorption leads to excited states that are substantially localized on either A or B, or causes an electron transfer from A to B (or *vice versa*). Moreover, because of its particular electron distribution, an excited molecule can associate with other species even when the ground state molecule does not exhibit this property. A particular case is that of an excited molecule that associates with a ground state molecule of the same chemical nature, forming an excited species $^*[A-A]$ which is called an *excimer* (from *excited dimer*). Association with a molecule of a different type leads to an *exciplex* (from *excited complex*). In suitably designed supramolecular systems, excimer and exciplex formation can be facilitated by preorganization of the structure. In more complex systems like dendrimers, it may happen that an excited unit is close to both a ground state unit of the same type and a ground state unit of a different type. Therefore, formation of both excimers and exciplexes can take place, resulting in three types of emission: monomer, excimer, and exciplex.¹⁰

2.1 Quenching processes in molecular and supramolecular systems

In fluid solutions, when intramolecular deactivation processes are not too fast, *i.e.* when the lifetime of the excited state is sufficiently long, an excited molecule *A may have a chance to encounter a molecule of another species, B. In such a case, some specific interaction can lead to the quenching of the excited state by second-order kinetic processes. The rate constant and the efficiency of the *A quenching process can be evaluated by eqn (1), the well-known Stern-Volmer equation, and (2), respectively:

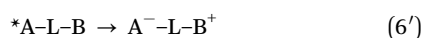
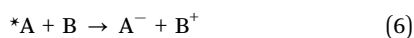
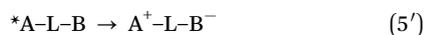
$$\tau^0/\tau = 1 + \tau^0 k_q[B] \quad (1)$$

$$\eta_q = k_q/(k_r + k_p + k_{nr} + k_q) = 1 - (\tau/\tau^0) \quad (2)$$

In supramolecular systems quenching processes are no longer limited by diffusion and take place by first-order kinetics; as a consequence they can also involve very short-lived excited states, contrary to what happens for separated molecules. In supramolecular systems, the quenching constant k_q can be evaluated by the following equation:

$$k_q = 1/\tau - 1/\tau^0 \quad (3)$$

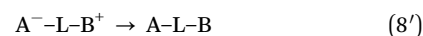
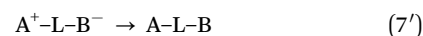
The two most important types of interaction of an excited state *A with another molecule B (free in solution or as a component of a supramolecular system) are *electron transfer* and *energy transfer* processes that can be summarized by eqn (4)–(6) and (4')–(6'), for molecular and supramolecular systems, respectively:



These processes are said to quench the excited state *A because they compete with the intramolecular deactivation paths of *A and therefore manifest themselves by quenching the *A luminescence (as well as any other intramolecular deactivation path of *A).

Energy transfer (eqn (4) and (4')) leads to the formation of an excited state (*B) of the quencher, which will then undergo its own deactivation processes, including luminescence (*sensitized luminescence*) and reaction (*sensitized reaction*).

Electron transfer may involve oxidation (eqn (5) and (5')) or reduction (eqn (6) and (6')) of the excited state. In the absence of subsequent chemical processes (*e.g.*, fast reaction of the oxidized and/or reduced species), the photoinduced electron-transfer processes are followed by spontaneous back electron-transfer reactions that regenerate the starting ground state systems (eqn (7), (8) and (7'), (8')).



Clearly, a crucial step in the design of a photoactive supramolecular system is the choice of the chromophores to be included in the components. Such a selection is made on the basis of the spectroscopic, photophysical, photochemical and redox parameters of the chromophores, depending on the intercomponent process(es) that have to be exploited for achieving the function desired for the supramolecular assembly. For example, as will be discussed in Section 4, the planning of photoinduced electron-transfer processes requires the knowledge of the excited state energy and electrochemical potentials of the partners involved. In most cases, the absence of photochemical side reactions (*e.g.*, decomposition) is an important requirement for a chromophore. A detailed evaluation of these aspects can be made on the basis of the mechanistic models available to interpret energy- and electron-transfer processes, which can be found in other references.⁹

3. Photoinduced energy transfer

Energy transfer can take place either by *radiative* or *non-radiative* processes. Non-radiative processes are the most interesting ones and two principal mechanisms are usually considered.⁹ The Coulombic mechanism (also called resonance, Förster-type (FRET), or through-space), is a long-range mechanism that does not require physical contact between donor and acceptor. The second mechanism is the exchange (also called Dexter-type) mechanism and its rate is exponentially dependent on distance.

Considering a supramolecular system in which the light absorbed by component A is followed by energy transfer to component B, and from B to a luminescent component C, the selective excitation of the A component results in the sensitized emission of C. The quantum yield of the sensitized emission of

Q6

C (Φ_{sens}), *i.e.* the number of photons emitted by C divided by the number of photons absorbed by A is given by eqn (9):

$$\Phi_{\text{sens}} = \eta_{\text{et}(*\text{A} \rightarrow \text{B})} \eta_{\text{et}(*\text{B} \rightarrow \text{C})} \Phi_{*C} \quad (9)$$

where Φ_{*C} is the intrinsic emission quantum yield of $*C$, *i.e.* the number of photons emitted by C divided by the number of photons absorbed directly by C, $\eta_{\text{et}(*\text{A} \rightarrow \text{B})}$ and $\eta_{\text{et}(*\text{B} \rightarrow \text{C})}$ are the efficiencies of energy transfer from $*A$ to B and from $*B$ to C, respectively. Where the excitation energy is used to drive a photoreaction or an electron transfer process, in eqn (9) the sensitized (Φ_{sens}) and intrinsic (Φ_{*C}) photoreaction or electron transfer quantum yield of C should be considered. Clearly, the quantum yield of the sensitized emission of C cannot be larger than the quantum yield of the emission obtained upon direct excitation of C.

3.1 Dendrimers as light-harvesting antennae

One of the most representative and instructive examples of multiple energy transfer processes in supramolecular systems is represented by light-harvesting antennae. Dendrimers^{11,12} are ideal scaffolds to build up molecular antennae:¹³ many photoactive units can be organized within a restricted space in predetermined sites of their architecture, namely periphery, branches or core. The dendritic structure allows the tuning of the distance and degree of interaction among the different functional units. Furthermore, owing to their three-dimensional structure, dendrimers exhibit internal dynamic cavities where ions or molecules can be hosted. Because of their proximity, the various functional groups of a dendrimer can easily form electronic interactions with one another, or with molecules or ions hosted in the dendritic cavities or associated on the dendrimer surface.¹⁴ Light harvesting in dendritic systems has also been coupled to rotaxane¹⁵ and discussed from a purely theoretical viewpoint.¹⁶

Dendrimer **1** (Fig. 1a) is constituted by a trimetallic nitride template endohedral metallofullerene linked to two oligo(phenylene-ethynylene) arms (hereafter called OPE).¹⁷ The emission spectrum of **1** in de-aerated toluene solution shows two bands: the first one at *ca.* 365 nm is centered on the OPE moiety and is strongly

quenched (>20 times) compared to the model compound, and the second one in the 680–900 nm region can be attributed to the fullerene core. The quenching of the OPE fluorescence can be attributed to a 100% efficient energy transfer (Fig. 1b). Indeed, the same fullerene emission intensity was recorded upon excitation of two iso-absorbing solutions of **1** at 320 nm, where most of the light is absorbed by the pending OPEs, and at 405 nm, where only the fullerene absorbs light. Therefore, the two OPE units act as extremely efficient light-harvesting antennae for the sensitization of the fullerene emission. Moreover, compared to the very weak fluorescence ($\Phi_{\text{em}} = 3 \times 10^{-4}$, $\tau = 1.5$ ns) typical of C_{60} , compound **1** exhibits outstanding luminescence properties in the near-IR region, even larger than the non-functionalized model $Y_3N@C_{80}$. Other properties of the luminescent excited state of **1** are: (i) slightly lower emission energy compared to the non-functionalized endohedral fullerene, (ii) relatively high quantum yield (0.08 in de-aerated solution), (iii) long lifetime (16 μs at 298 K – 20 times longer than $Y_3N@C_{80}$ – and 13 ms at 77 K), and (iv) high sensitivity to the presence of dioxygen in fluid solution. Dioxygen efficiently quenches the emission of **1** in solution with a rate constant $k_q = 8 \times 10^8 \text{ M}^{-1} \text{ s}^{-1}$. Quenching by dioxygen (Fig. 1b) leads to sensitization of 1O_2 emission at 1270 nm with a quantum yield of 1.0 and 0.7 for **1** and $Y_3N@C_{80}$, respectively.

Dendrimer **1** also shows interesting liquid crystalline behaviour: the grafting of the mesomorphic OPE arms onto the fullerene core promotes mesomorphism, with the induction of columnar phases. The luminescence properties are retained in the mesophase and, coupled with quite strong absorption in the visible region extending up to 750 nm, open up a variety of applications, ranging from photovoltaics to near-IR luminescent sensors with time-gated detection to shut down fluorescence of the matrix or competing species.

3.2 Dendrimers for energy upconversion

Dendrimers can be exploited not only to obtain light-harvesting antennae in which the emitted photons are at lower energy than

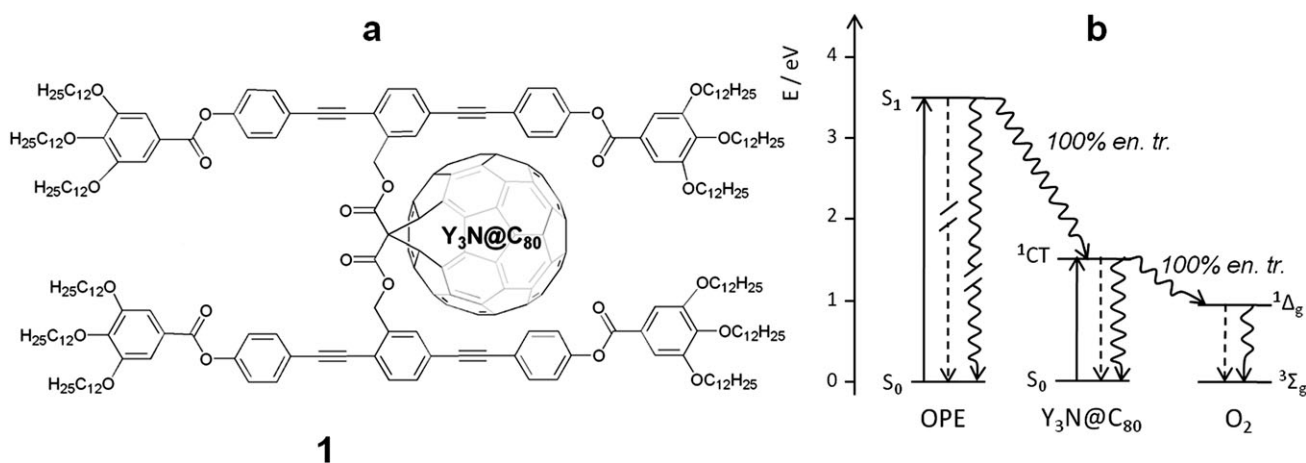
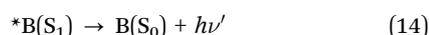
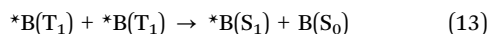
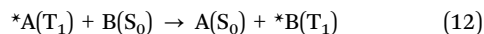
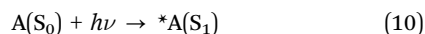


Fig. 1 Structure of dendrimer **1** (a) and energy level diagram (b) showing the excited states involved in the main photophysical processes (excitation: solid lines; radiative deactivation: dashed lines; non-radiative deactivation processes: wavy lines).¹⁷

the absorbed ones, as in the case of dendrimer **1**, but also to get energy upconversion, in which incident photons of a given energy are converted into photons of higher energy. Among the different approaches to energy upconversion, the one described here is based on sensitized triplet-triplet annihilation, which can be performed by low power and incoherent excitation sources. Before describing the dendritic system, a few basic concepts on the working principle of upconversion by triplet-triplet annihilation will be recalled.

This process was first reported in the '60s by Parker *et al.*¹⁸ with organic chromophores absorbing and emitting in the UV region. It remained a curiosity for photochemists up to a few years ago because of the low efficiency of the process coupled with the low photostability of the employed chromophores. More recently, Castellano *et al.* reported the use of metal complexes as triplet sensitizers, thus increasing the photostability of the chromophores and the efficiency of the process. In this case, upconverted emission is visible with the naked eye by excitation with a commercial green laser pointer at low power (<5 mW at 532 nm).¹⁹ The increasing interest in the topic is driven by applications: wavelength shifting for spectroscopy, sensitized photoreaction by low-energy photons, photovoltaic devices, and luminescent probes for bioimaging.^{20,21}

The working principle is described by eqn (10)–(14) involving two chromophores A and B characterized by the energy level pattern as depicted in Fig. 2.



The energy requirements of the two partners are: (i) the S_1 excited state of B is at a higher energy than that of A, while the

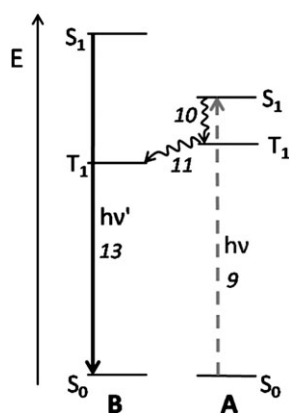


Fig. 2 Energy level diagram for an upconversion system based on triplet-triplet annihilation. For clarity purposes, only the processes related to the upconversion phenomenon are reported: absorption (dashed line), non-radiative processes (wavy lines), fluorescence (solid line). The numbers on the arrows refer to those of the equations in the text.

corresponding T_1 excited states are in the reverse order, (ii) the combined triplet energy of ${}^*B(T_1)$ is greater than or equal to the energy of ${}^*B(S_1)$. The energy difference between S_1 and T_1 of B should be as high as possible, while the S_1 and T_1 excited states of A should be as close as possible in energy. In this way, you can reach the highest energy difference between the exciting and emitted photons. To guide the choice of the chromophores, besides the energetic requirement, key features are the unitary efficiency of the $S_1 \rightarrow T_1$ inter system crossing and long lifetimes of the T_1 excited states of both A and B.

To move towards applications, solid state devices are preferable to solution-based ones. However, the process described so far relies on dynamic processes 12 and 13, which require the encounter of molecules. Therefore, this mechanism works only if a certain degree of translational mobility is assured, as demonstrated by experiments at 77 K where no emission is observed. In a rubbery polymer matrix, above the glass transition temperature of the polymer,²⁰ the upconversion quantum yields are much lower and depend on the viscosity of the matrix.

Another approach towards solid-state devices is to covalently link A to several B chromophoric units in a dendritic structure, so that the energy transfer process 12 and triplet-triplet annihilation 13 are no longer dynamic processes and the system can work in conditions where translational mobility is blocked, like conventional solid state devices.

A recent example is dendrimer **2** (Fig. 3a) which consists of a $[Ru(bpy)_3]^{2+}$ (bpy = 2,2'-bipyridine) complex as the core and four diphenylanthracene (hereafter called DPA) units at the periphery.²² Upon excitation at 373 nm, most of the light (*ca.* 85%) is absorbed by DPA, two emission bands are observed due to the fluorescence of DPA at 410 nm and the phosphorescence of the Ru(II) complex at *ca.* 620 nm. The luminescence results show that the $S_1(\pi\pi^*)$ excited state of the peripheral DPA units of dendrimer **2** is quenched more than 40 times the model compound by energy and electron transfer processes involving the Ru(II) complex. The $[Ru(bpy)_3]^{2+}$ phosphorescence is quenched 10 times more due to energy transfer from 3MLCT to populate the $T_1(\pi\pi^*)$ excited state of the DPA units with a 90% efficiency (Fig. 3b).

At 77 K in a 1 : 1 (v/v) $C_2H_5OH-CH_2Cl_2$ rigid matrix, quenching of the $S_1(\pi\pi^*)$ excited state of the peripheral DPA units is less efficient because electron transfer is precluded as a result of the destabilization of the CT level at 77 K due to the lack of solvent repolarization.

Upon laser excitation of a de-aerated solution of dendrimer **2** at 532 nm, where mainly $[Ru(bpy)_3]^{2+}$ absorbs, fluorescence of DPA at 410 nm is observed both at 298 K in CH_3CN and at 77 K in the 1 : 1 (v/v) $C_2H_5OH-CH_2Cl_2$ rigid matrix. The corresponding decay time is much longer (μs -time scale in both cases) than that observed by direct excitation of the DPA units (<0.5 ns). This finding is due to the delayed fluorescence of DPA obtained by an energy up-conversion mechanism: excitation at 532 nm yields emission at 410 nm.

In fluid solution, the two separated chromophores in the de-aerated solution show a much higher upconverted emission intensity than their dendritic assembly because the quenching

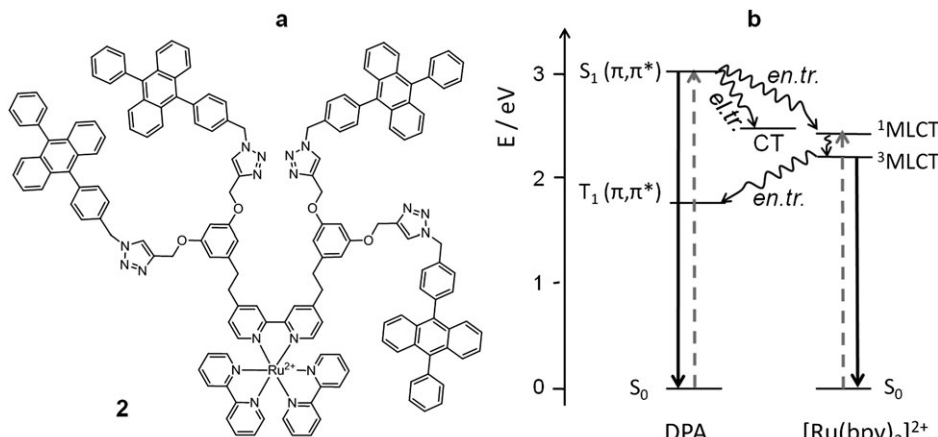


Fig. 3 Structure of dendrimer **2** (a) and energy level diagram (b) showing the excited states involved in the main photophysical processes (excitation: gray dashed lines; radiative deactivation: solid lines; non-radiative deactivation processes: wavy lines).²²

of the upconverted fluorescence of DPA to a nearby Ru(II) complex can occur in the dendrimer but not in the solution containing the separated chromophores. Indeed, the lifetime of the S_1 excited state of DPA is too short to be dynamically quenched by the Ru(II) complex at the concentration used. On the other hand, on freezing the solution at 77 K, only the dendrimer shows upconverted emission and the quenching of the DPA fluorescent excited state is greatly reduced by prevention of electron transfer processes.

For future developments, an increase in the efficiency of energy upconversion in the solid matrix by multichromophoric systems is desirable. This can be pursued by optimizing the distance between the absorbing chromophore A and the emitting chromophore B to have a sufficiently fast rate of process 12 and a slow energy transfer between $*B(S_1)$ and $A(S_0)$.

4. Photoinduced electron transfer

The relevant excited-state thermodynamic properties for photoinduced electron-transfer processes are the reduction potentials of the couples $A^+/*A$ (eqn (5) and (5')) and $*A/A^-$ (eqn (6) and (6')). It should be recalled that, because of its higher energy content, an excited state is both a stronger reductant and a stronger oxidant than the corresponding ground state.⁹ To a first approximation, the redox potentials of the excited state couples can be calculated from the potentials of the ground state couples and the one-electron potential corresponding to the zero-zero excitation energy (eqn (15) and (16)):

$$E(A^+/*A) \approx E(A^+/A) - E_{0-0} \quad (15)$$

$$E(*A/A^-) \approx E(A/A^-) + E_{0-0} \quad (16)$$

Therefore, the Gibbs free energy for the photoinduced electron-transfer processes schematized in eqn (5) (or 5') and 6 (or 6') can be respectively estimated on the basis of eqn (17) and (18):²³

$$\Delta G_{et}^o \approx N_A \{ e[E(A^+/A^-) - E(B/B^-)] + w(A^+B^-) \} - E_{0-0} \quad (17)$$

$$\Delta G_{et}^o \approx N_A \{ e[E(A/A^-) - E(B^+/B)] + w(A^-B^+) \} - E_{0-0} \quad (18)$$

in which N_A is Avogadro's number, e is the electronic charge, and w is the electrostatic work term that accounts for the Coulombic interactions between the partners after electron transfer.

In a supramolecular system, both photoinduced and back (thermal) electron-transfer processes can be viewed as non-radiative transitions between different, weakly interacting electronic states of the A–L–B species. From a kinetic viewpoint, these processes can be dealt with in the framework of Marcus theory and successive more refined models. More details can be found in ref. 24.

Photoinduced electron-transfer processes have been widely investigated in supramolecular chemistry, particularly with the aim of developing light-powered molecular wires, switches, and charge-separation devices.⁶ Indeed, photoinduced electron transfer reactions convert light energy into an electrochemical potential, a feature that is at the basis of both natural and artificial photosynthetic systems.²⁵

4.1 Photoinduced electron transfer in multichromophoric rotaxanes

Rotaxanes are mechanically interlocked compounds which minimally consist of an axle-type molecule surrounded by a macrocyclic ring and terminated with bulky stoppers that prevent dethreading of the two components.²⁶ Taking advantage of the fact that²⁴ crown-8-type macrocycles can form hydrogen-bonded inclusion complexes with 1,2-bis(pyridinium)ethane guests,²⁷ rotaxanes based on such a recognition motif and containing a terminal terpyridine (tpy) group for coordination to a transition metal ion on their axle component have been prepared. These rotaxane ligands have been utilised in the preparation of a series of heteroleptic $[(tpy)Ru(tpy\text{-}rotaxane)]^{2+}$ complexes.²⁸ The investigated rotaxanes 5^{5+} – 7^{5+} , their axle component 4^{5+} , and the model compound for the Ru-based unit 3^{3+} , are shown in Fig. 4a. It should be noted that these compounds are in fact multichromophoric systems that contain several different units capable of interacting with one another and providing an interesting combination of structural features and photophysical properties.

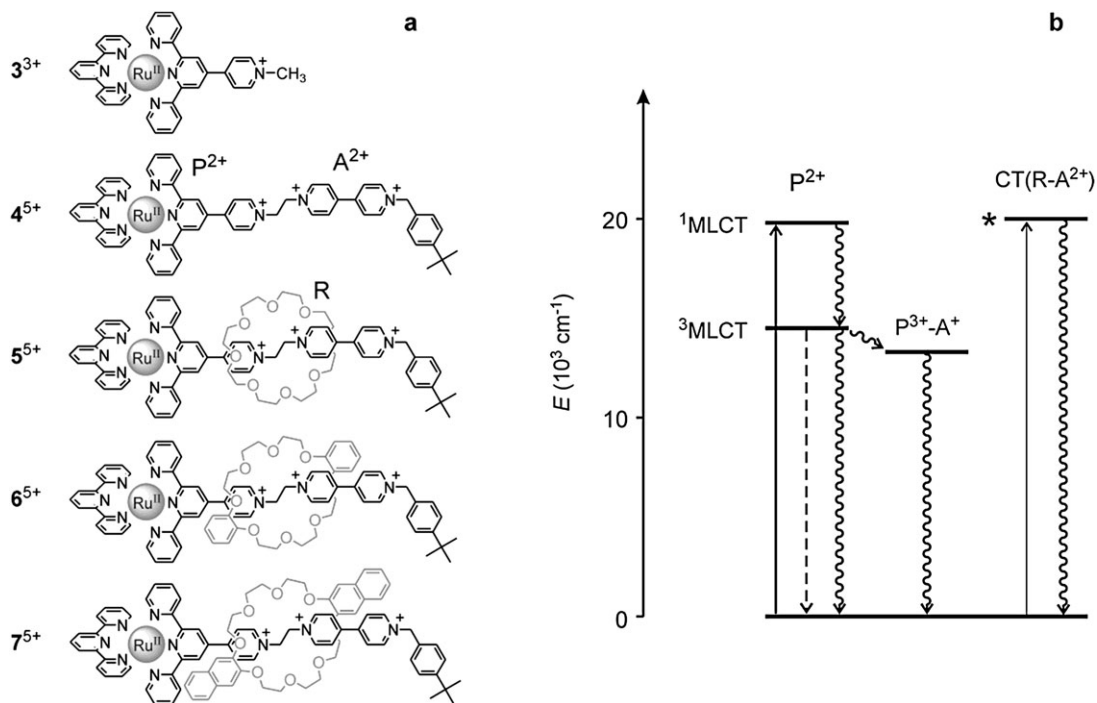


Fig. 4 (a) Structural formulas of the model compound 3^{3+} , axle species 4^{5+} , and multicomponent rotaxanes 5^{5+} – 7^{5+} . (b) Simplified energy-level diagram for the rotaxanes, in which the Ru-based photosensitizing unit, the 4,4'-bipyridinium electron acceptor and the macrocyclic ring are denoted as P^{2+} , A^{2+} and R, respectively. The observed absorption (full lines), emission (dashed lines) and non-radiative (wavy lines) processes are indicated. The level marked with an asterisk is observed only for rotaxanes 6^{5+} and 7^{5+} . The energy of the MLCT and CT levels were estimated from spectroscopic data, whereas that of the P^{3+} – A^+ state was calculated from electrochemical data using eqn (17).

At room temperature in CH_3CN , compound 3^{3+} exhibits a luminescence band in the far red ($\lambda_{\text{max}} = 775 \text{ nm}$) and a relatively long lived ($\tau = 125 \text{ ns}$) triplet MLCT excited state, whereas the parent $[\text{Ru}(\text{tpy})_2]^{2+}$ does not show an appreciable luminescence under the same conditions. This difference is due to the presence of a strong electron withdrawing pyridinium substituent on one of the two tpy ligands.²⁹ Visible light excitation of the Ru-based chromophore (P^{2+}) in complexes 4^{3+} – 7^{5+} causes a partial quenching of the MLCT luminescence because of an electron transfer to the 4,4'-bipyridinium unit (A^{2+}) of the axle component (P^{3+} – A^+ level in Fig. 4b). The quenching rate constants can be calculated by means of eqn (3), in which τ is the luminescence lifetime of the Ru-centered emission in compounds 4^{3+} – 7^{5+} and τ^0 is the lifetime value of the same emission in the absence of the bipyridinium quencher (*i.e.*, that of model 3^{3+}). For example, in the case of 4^{5+} , $k_q = 1.0 \times 10^8 \text{ s}^{-1}$.

The rotaxane structure affects the absorption and luminescence properties of the complexes. In particular, for compounds 6^{5+} and 7^{5+} a weak absorption tail that reaches down to 600 nm ($\epsilon \approx 500 \text{ M}^{-1} \text{ cm}^{-1}$ at 450 nm) is observed. Such a band is assigned to π -donor-acceptor interactions between the electron rich dioxyaromatic units of the macrocycles and the electron poor pyridinium and 4,4'-bipyridinium units of the cationic axle (CT(R - A^{2+}) level in Fig. 4b). Interestingly, when a crown ether surrounds the cationic thread the luminescence quenching process is slowed down by a factor of between 2 and 3, an effect attributed to the presence of the macrocycle in the rotaxane complexes which prevents the formation of folded conformations.

The excited state obtained upon photoinduced electron transfer can relax to the ground state by a back electron-transfer process. The fact that the electron-transfer state cannot be detected by transient absorption experiments suggests that the decay of such a state is faster than its formation, thereby preventing its accumulation after light excitation.

4.2 Autonomous molecular shuttling powered by visible light

A remarkable example of the utility of photoinduced electron transfer to bring about sophisticated functionalities in supramolecular species is represented by compound 8^{6+} in Fig. 5.³⁰

In this rotaxane the macrocycle can be positioned at a specific location along the axle-type (dumbbell) molecule by taking advantage of non-covalent interactions between the components and, if no substantial steric barriers are present, the macrocycle can displace itself along the axle, giving rise to a translational motion that resembles the displacement of a shuttle train along its railroad track.³¹ In fact, rotaxanes of this type are termed molecular shuttles and constitute simple examples of mechanical molecular machines.^{6–8}

Building upon experience gained with model systems,^{32,33} rotaxane 8^{6+} (Fig. 5) was specifically designed to achieve photoinduced ring shuttling in solution.³⁰ This compound has a modular structure; its ring component R is a π -electron-donating bis-*p*-phenylene-34-crown-10, whereas its dumbbell component is made of several covalently linked units. They are a Ru(II) polypyridine complex (P^{2+}), a *p*-terphenyl-type rigid spacer (S), a 4,4'-bipyridinium (A_1^{2+}) and a 3,3'-dimethyl-4,4'-bipyridinium

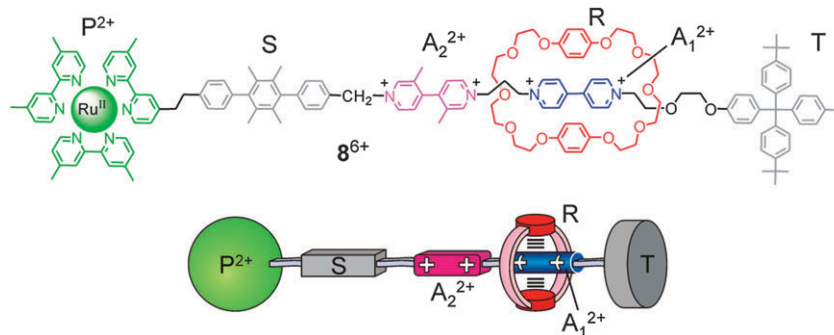


Fig. 5 Structural formula and cartoon representation of the [2]rotaxane 8^{6+} .^{30,34}

(A_2^{2+}) π -electron-accepting station, and a tetraarylmethane group as the terminal stopper (T). The Ru-based unit plays the dual role of a light-fueled power station and a stopper, whereas the mechanical switch consists of the two electron-accepting stations and the electron-donating macrocycle. Six PF_6^- ions are present as the counteranions of the positively charged rotaxane. The electron donor ring can establish charge-transfer interactions with both the A_1^{2+} and A_2^{2+} electron poor units of the axle; however, as the former site is a much better electron acceptor than the latter, the R component selectively encircles the A_1^{2+} unit (Fig. 5).

The strategy devised in order to obtain the photoinduced shuttling movement of R between the two stations A_1^{2+} and A_2^{2+} is based on a “four stroke” synchronized sequence of electron-transfer and molecular rearrangement processes, as illustrated in the central part of Fig. 6.^{30,34,35} Visible light excitation of 8^{6+} (process (1)) generates the lowest singlet excited state ($^1\text{MLCT}$) of the P^{2+} unit, which quickly deactivates to the lower lying triplet state ($^3\text{MLCT}$). Such a triplet is relatively long lived ($\approx 1 \mu\text{s}$ in deoxygenated solution at room temperature) and the redox potential for its oxidation is about -0.8 V versus SCE.

Since the one-electron reduction of A_1^{2+} occurs at *ca.* -0.4 V versus SCE, the transfer of an electron from the $^*\text{P}^{2+}$ unit to A_1^{2+} (process 2) is thermodynamically downhill. Such a reaction competes with the intrinsic decay of the P^{2+} excited state (process 3).

After the reduction of A_1^{2+} , with the consequent “deactivation” of this site, the ring moves (process 4) by 1.3 nm to encircle A_2^{2+} , a step that is in competition with the back electron-transfer from A_1^+ (still encircled by R) to the oxidized unit P^{3+} (process 5). Eventually, a back electron-transfer from the “free” reduced site A_1^+ to the oxidized unit P^{3+} (process 6) restores the electron acceptor power to this radical cationic unit. As a consequence of the electronic reset, thermally activated back movement of the ring from A_2^{2+} to A_1^{2+} takes place (process 7).

Steady-state and time-resolved spectroscopic experiments complemented by electrochemical measurements in acetonitrile solution, demonstrated that the absorption of a visible photon by 8^{6+} can cause the occurrence of a forward and backward ring movement, that is, a full mechanical cycle according to the mechanism illustrated in the central part of Fig. 6.³⁴ The energy levels involved in the photoinduced ring shuttling are shown

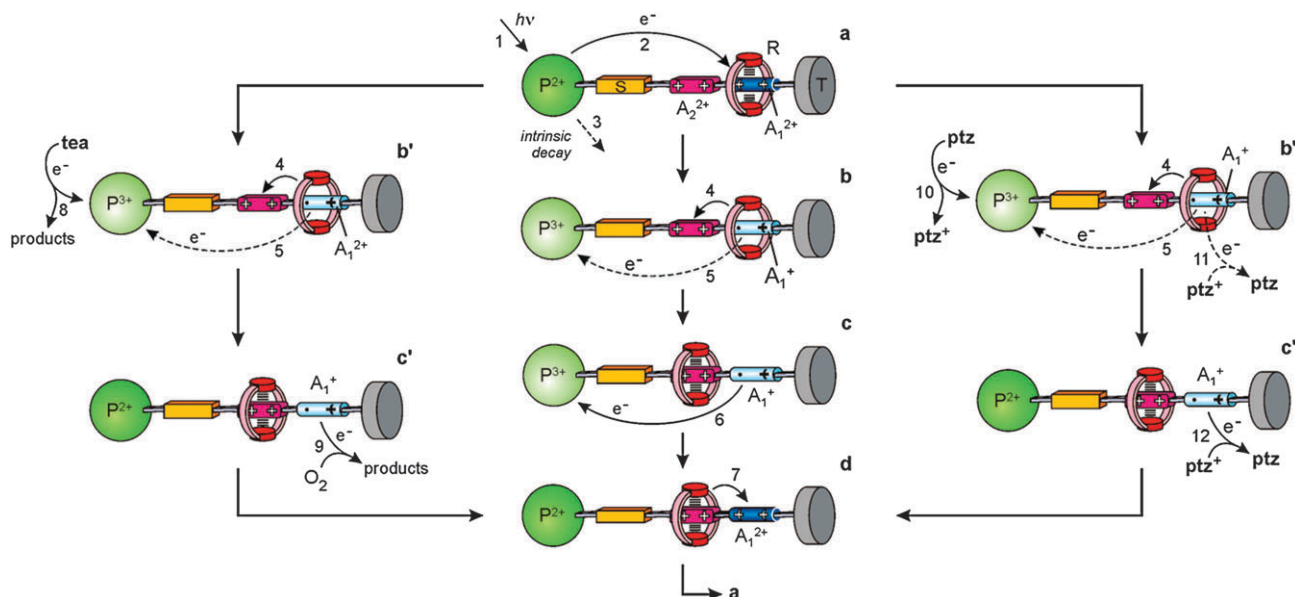


Fig. 6 Schematic representation of the photochemically driven ring shuttling in rotaxane 8^{6+} . Left: shuttling assisted by two sacrificial fuels. Centre: autonomous operation based on intramolecular processes. Right: autonomous operation assisted by an electron relay.³⁴

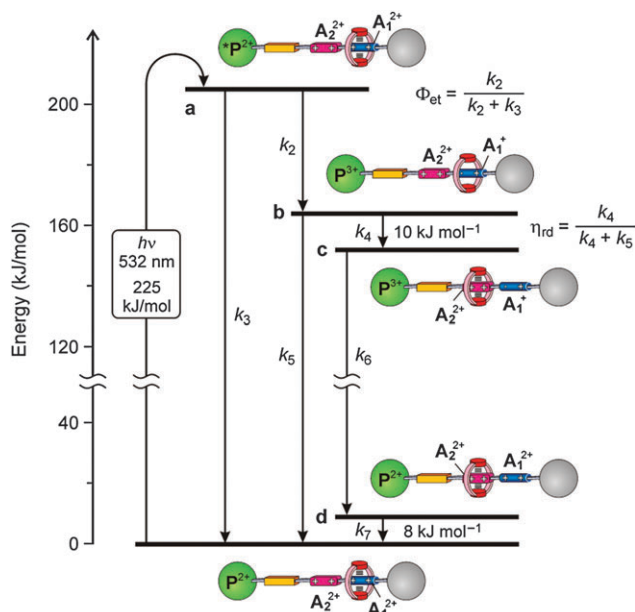


Fig. 7 Energy level diagram for the processes taking place in rotaxane $\mathbf{8}^{6+}$ when it works as a light-driven molecular shuttle based on intramolecular processes at room temperature. Levels (a–d) correspond to the states shown in Fig. 6, centre.

in Fig. 7. The key issues of this mechanism are the competition between processes 2 (photoinduced electron transfer) and 3 (intrinsic excited-state deactivation), and between processes 4 (ring displacement from the reduced A_1^+ site) and 5 (back electron transfer). Luminescence measurements showed³⁰ that the rate constants of processes 2 and 3 at 303 K are $k_2 = 2.5 \times 10^5 \text{ s}^{-1}$ and $k_3 = 1.3 \times 10^6 \text{ s}^{-1}$, respectively, corresponding to a quantum yield for the electron-transfer process $\Phi_{\text{et}} = k_2/(k_2 + k_3) = 0.16$. The time constants of processes 4 and 5, which are respectively $k_4 = 2.1 \times 10^4 \text{ s}^{-1}$ and $k_5 = 1.5 \times 10^5 \text{ s}^{-1}$ at 303 K, were determined by transient absorption spectroscopy.^{30,34} Hence, the efficiency of ring displacement from the photo-reduced A_1 station is $\eta_{\text{rd}} = k_4/(k_4 + k_5) = 0.12$; because all the successive processes have no competitors, the overall shuttling quantum yield is simply $\Phi_{\text{sh}} = 0.16 \times 0.12 = 0.02$. Thermodynamic considerations³⁴ show that the energy available for the forward and backward ring shuttling reactions (processes 4 and 7, respectively, in Fig. 6 and 7) are 10 and 8 kJ mol^{-1} , respectively. Hence, the fraction F of the excited state energy (205 kJ mol^{-1}) used for the motion of the ring amounts to *ca.* 10%, and the overall efficiency of the machine is $\eta = \Phi_{\text{sh}} \times F = 0.2\%$.

This somewhat disappointing result is compensated by the fact that the investigated system gathers together the following features: (i) it is powered by visible light (in other words, sunlight); (ii) it exhibits autonomous behavior (*i.e.*, like natural molecular motors, it operates automatically in a constant environment as long as the energy source is available); (iii) it does not generate waste products; (iv) its operation can rely only on intramolecular processes, allowing in principle operation at the single-molecule level; (v) it can be driven at a frequency of about 1 kHz; (vi) it works in mild environmental

conditions (*i.e.*, fluid solution at ambient temperature); and (vii) it is stable for at least 10^3 cycles.

Calculations of the free energy profile for the electronic ground state and the electron-transfer state afforded by photoexcitation of $\mathbf{8}^{6+}$ as a function of the position of the ring along the axle revealed that both the forward and back shuttling movements appear to be almost barrierless, with predicted time constants in the nanosecond range; barriers, however, appear if the detachment of the PF_6^- counteranions from the station that has to receive the ring is taken into consideration.³⁶

The molecular shuttle $\mathbf{8}^{6+}$ can also be operated, with a higher quantum yield, by a sacrificial mechanism³⁰ based on the participation of external reducing (triethanolamine, **tea**) and oxidizing (O_2) species (Fig. 6, left), and by an intermolecular mechanism³⁴ involving the kinetic assistance of an external electron relay (phenothiazine, **ptz**), which is not consumed (Fig. 6, right). However, operation by the sacrificial mechanism does not afford autonomous behavior and leads to consumption of chemical fuels and formation of waste products. On the other hand, the assistance by an electron relay affords autonomous operation in which only photons are consumed, but the mechanism is no longer based solely on intra-rotaxane processes.

5. Photoisomerization

Photoisomerization refers to the transformation of a compound from one isomeric form to another caused by light irradiation.³⁷ In most instances, the interconvertible forms are *cis-trans* stereoisomers or ring open–closed structures. A prototypical case of photoisomerization is the light-induced *trans* \rightarrow *cis* transformation of the $-\text{N}=\text{N}-$ double bond in azobenzene (Fig. 8). This reaction is extremely fast, efficient, clean and reversible, and the two isomers exhibit quite different structures and properties.³⁸ Therefore, such a process is ideal to introduce light-driven functionalities in suitably designed molecular and supramolecular systems in order to develop photochemical devices³⁹ and materials.⁴⁰ As a matter of fact, molecular tweezers based on the azobenzene unit were the first examples of light-driven molecular machines reported in the literature⁴¹ and nowadays have reached a high level of sophistication,⁴² as exemplified by the behavior of the system described below.

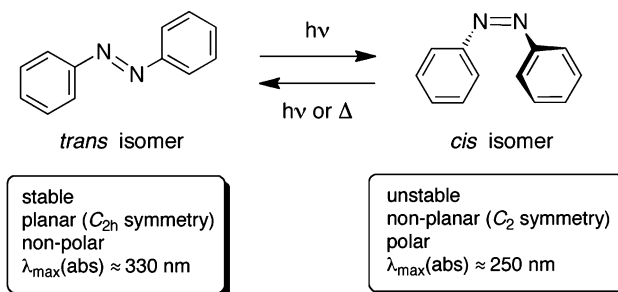


Fig. 8 The photoisomerization of azobenzene.

5.1 A dendrimer coupling photocontrolled tweezer function with light harvesting capability

Compound **9** (Fig. 9) is a small dendrimer that contains three completely different types of components: six naphthyl chromophoric moieties, an azobenzene photochromic group, and two cyclam units.⁴³ Taken separately, each type of component has its own properties: (a) the naphthyl chromophoric units exhibit an absorption band at 275 nm and a fluorescence band at 335 nm, (b) the azobenzene photochromic unit has absorption bands at 366 and 450 nm and can be switched from the *trans* to the *cis* form by light excitation, and (c) cyclam is one of the most extensively investigated ligands in coordination chemistry; it does not show absorption bands in the visible region and its amine groups can play the role of electron donors towards aromatic molecules like naphthalene.

In compound **9** (shown as the *trans* isomer) there are several types of interactions among the different components. In CH₃CN–CH₂Cl₂ solution, the naphthyl localized emission at 335 nm is much weaker than in model naphthyl molecules and is accompanied by an emission at 470 nm from the naphthyl-amine exciplexes. The *trans* → *cis* isomerization of the azobenzene unit takes place upon excitation in the azobenzene band at 366 nm and also *via* energy transfer (20% efficiency) from the naphthyl groups, showing that the naphthyl branches play a light harvesting role towards the azobenzene switching.

The coordination ability of the two cyclam units can then be exploited to modify the functions of **9** and to perform new ones.

Since the two cyclam units are linked by azobenzene that can be switched from the *trans* to the *cis* form by light excitation, their distance can be light controlled. In the initial, extended *trans* form each cyclam coordinates a metal ion. The compounds [Zn₂**9**]⁴⁺ and [Cu₂**9**]⁴⁺ can thus be prepared in solution. In [Zn₂**9**]⁴⁺, the emission band at 470 nm is no longer observed, as expected because coordination of Zn(II) to the cyclam amine groups prevents exciplex formation. In agreement with the lack of deactivation *via* exciplex formation, the naphthyl-sensitized *trans* → *cis* isomerization of azobenzene occurs with 100% efficiency.

In the *cis* form, the two cyclam units face each other and coordinate only one metal ion. Therefore the *trans* → *cis* azobenzene isomerization in [Zn₂**9**]⁴⁺ leads to the release of a Zn²⁺ ion. Thus, in *trans*-[Zn₂**9**]⁴⁺ light harvesting by the naphthyl units through the sensitized isomerization of azobenzene controls metal ion coordination. In *trans*-[Cu₂**9**]⁴⁺, the situation is reversed: metal coordination controls photoisomerization. The naphthyl excited states are quenched by energy or electron transfer processes involving the Cu²⁺ metal ion, as shown by the absence of any fluorescence, so that the naphthyl sensitized isomerization of the azobenzene unit does not take place.

The functions performed by the three types of components of **9**, namely the two cyclam coordinating sites, the photoisomerizable azobenzene core, and six light-harvesting naphthyl units, cooperate or interfere depending on the nature of the metal ion (Fig. 10): Zn²⁺ coordination allows a 100% efficient sensitization of *trans*-azobenzene by the light-harvesting naphthyl antenna,

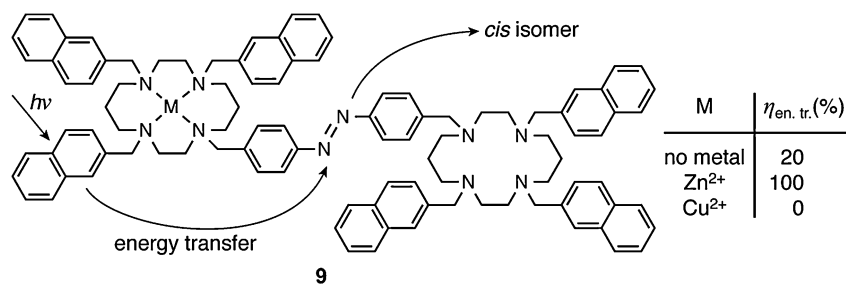


Fig. 9 Structural formula and relevant photoinduced processes of *trans* compound **9**.⁴³

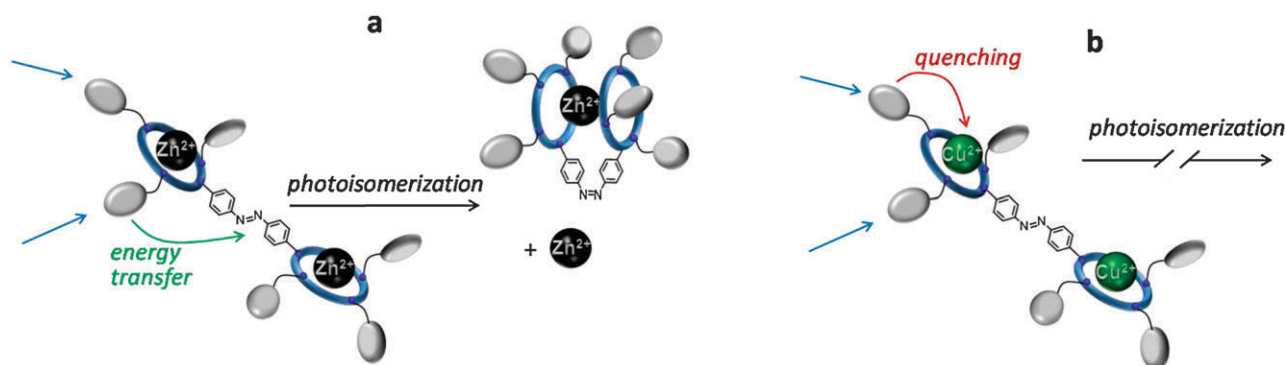


Fig. 10 Schematic representation of the functions performed by dendrimer **9**: different coordination ability by the cyclam moieties (blue circles) as *trans* and *cis* isomers, light-harvesting by naphthalene units (grey ovals) and sensitized photoisomerization of the azobenzene core for Zn²⁺ (a) and Cu²⁺ metal complexes (b).

whereas Cu^{2+} prevents this effect. Furthermore, a Zn^{2+} ion can be released in solution upon the photochemical isomerization of $[\text{Zn}_2\mathbf{9}]^{4+}$, whereas this process is not available to $[\text{Cu}_2\mathbf{9}]^{4+}$.

Compared to the pioneering work on azobenzene-based photoresponsive crown ethers,⁴¹ compound **9** exhibits a much more complex behavior coupling the photocontrolled tweezer function with the light harvesting antenna performed by the naphthyl moieties and the possibility to switch ON/OFF the sensitization of azobenzene depending on the nature of the coordinated metal ion. The cyclam moieties cannot discriminate between Zn^{2+} and Cu^{2+} ions, but the resulting complexes can be differentiated on the basis of their photochemical behavior. A Cu^{2+} -like behavior is expected for all metal ions exhibiting low-lying excited states or that are easy to oxidize and reduce and can quench naphthalene by energy or electron transfer.

5.2 A molecular machine exhibiting a photoinduced memory effect

A recently reported sophisticated supramolecular system in which azobenzene photoisomerization plays a crucial role is the [2]rotaxane $\mathbf{10}^{4+}$ shown in Fig. 11.⁴⁴

In this species, orthogonal chemical and photochemical stimuli are used to gain full control of the thermodynamics (*i.e.*, the distribution of the rings between the two sites located along the axle) and the kinetics (*i.e.*, the translation rate of the rings between the sites) of molecular shuttling. A system of this kind is interesting not only from the view point of molecular machines but also for that of signal processing and storage. As a matter of fact, controllable molecular shuttles can be considered as bistable mechanical switches at the nanoscale. While the operation of bistable molecular switches is based on classical switching processes between thermodynamically stable states, the development of molecular memories – which rely on a sequential logic behavior⁶ – also requires a control of the rates of the mechanical movement between such states.

The functional units incorporated in $\mathbf{10}^{4+}$ (Fig. 11) are: (i) a π -electron-deficient ring; (ii) the π -electron donor recognition sites of the dumbbell component, constituted by a tetrathiafulvalene (TTF) unit and a 1,5-dioxynaphthalene (DNP) unit; and (iii) a photoactive 3,5,3',5'-tetramethylazobenzene (TMeAB) moiety, located in between the TTF and DNP units, which can be reversibly and efficiently switched between its *trans* and *cis* configurations by photochemical stimuli. Since the TTF unit is more π -electron rich than the DNP one, the macrocycle prefers to encircle the TTF unit rather than the DNP one in the starting co-conformation of $\mathbf{10}^{4+}$ (Fig. 12).

This preference is evidenced by the presence of a charge-transfer absorption band peaking at 850 nm. Upon chemical or electrochemical oxidation of the TTF unit to its radical cation ($\text{TTF}^{\bullet+}$) form, signalled by the appearance of the $\text{TTF}^{\bullet+}$ absorption features in the 400–650 nm region, the macrocycle shuttles to the DNP recognition site on account of the electrostatic repulsion caused by the $\text{TTF}^{\bullet+}$ radical cation and the loss of π -donor-acceptor interactions with the ring. Such a process can be monitored by the disappearance of both the band at 850 nm and the sharp absorption features at around 320 nm, typical of the DNP site not surrounded by the macrocyclic ring.

Steady state and time-resolved UV-visible spectroscopic experiments showed that upon the quick chemical reduction of the $\text{TTF}^{\bullet+}$ unit to its neutral state the ring immediately shuttles back to encircle the TTF site if the TMeAB unit is in the *trans* configuration, whereas it remains trapped on the DNP site if the TMeAB unit has been photoisomerized to the *cis* isomer prior to the $\text{TTF}^{\bullet+} \rightarrow \text{TTF}$ back reduction (Fig. 12). Indeed, the first-order rate constant for replacement of the ring onto the regenerated TTF site in the photoisomerized rotaxane, obtained by monitoring the recovery of the charge-transfer absorption band at 850 nm, is in very good agreement with the first-order rate constant corresponding to the thermal *cis* \rightarrow *trans* isomerization of the TMeAB unit, measured by observing the recovery of the absorption band of the *trans*-TMeAB unit at 344 nm (Fig. 13).

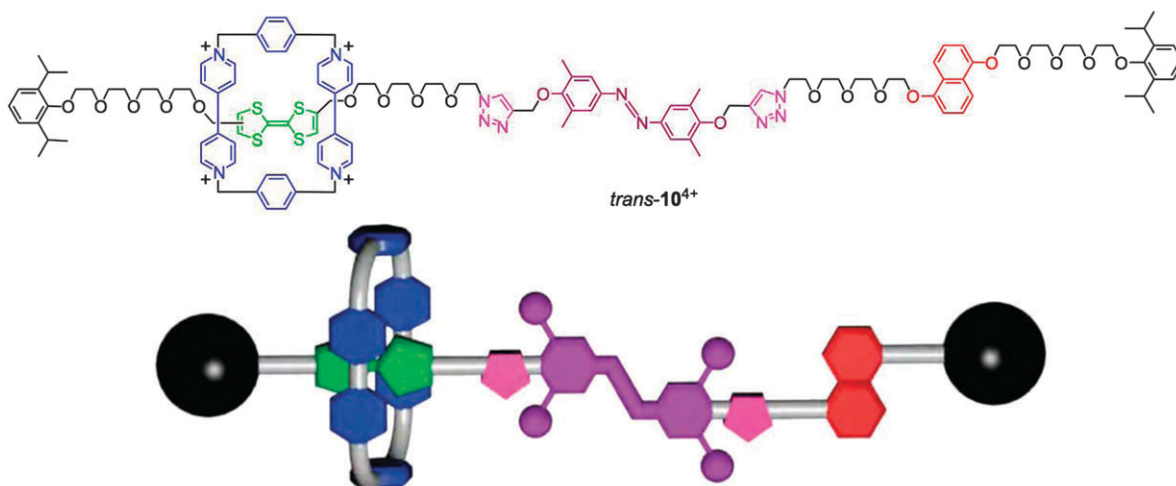


Fig. 11 Structural formula and cartoon representation of the [2]rotaxane $\mathbf{10}^{4+}$ in the *trans* isomer.⁴⁴

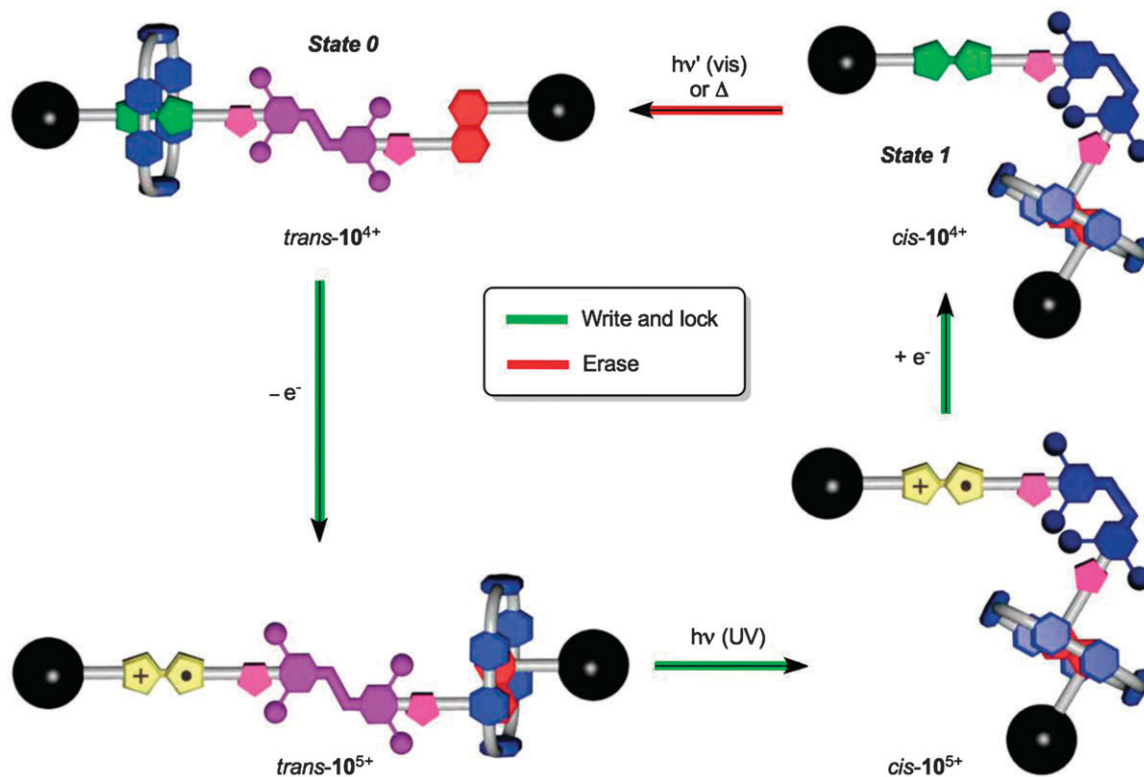


Fig. 12 Chemically and photochemically triggered memory switching cycle of rotaxane 10^{4+} .⁴⁴

This behavior can be explained by considering that the *trans* \rightarrow *cis* isomerization of TMeAB brings about a large geometrical change capable of substantially affecting the free-energy barrier for the shuttling of the macrocycle along the axle component. The *cis*-azobenzene unit indeed poses a much larger steric hindrance to ring shuttling than the *trans* isomer.

In summary, the switching cycle of rotaxane 10^{4+} (Fig. 12) consists of the following steps: (i) oxidation of TTF, causing ring shuttling from the TTF $^{*+}$ to the DNP site; (ii) UV light irradiation, converting the TMeAB unit from the *trans* to the *cis* configuration (gate closed); (iii) back reduction, regenerating the neutral TTF unit with the ring still residing on the DNP unit, and (iv) successive photochemical or thermal *cis* \rightarrow *trans* back isomerization, opening the gate and enabling the replacement of the macrocycle onto the TTF primary recognition site.

In other words, in a “write–lock–erase” experiment based on the cycle shown in Fig. 12 the data is written on the rotaxane by an oxidation stimulus, and locked by UV light irradiation; after the writing session, the oxidized species can be reduced back to the original form without losing the written data for a remarkably longer time compared to thermodynamically controlled molecular switches. Indeed, the data remain stored for a few hours in the dark at room temperature until the thermal opening of the azobenzene gate occurs. Therefore, 10^{4+} operates as a bistable memory element under light-triggered kinetic control. It is also important to note that light irradiation not only locks the data previously recorded by oxidation, but also protects the non-oxidized rotaxanes from accidental writing.

6. Photoinduced proton transfer

As discussed earlier, the electronically excited states of a chemical species usually have quite different properties in comparison to the ground state. If a molecule possesses an acid (or basic) site, it often happens that its pK_a (or pK_b) value changes upon photoexcitation. This property opens up the possibility of triggering proton transfer reactions in solution by light. As for bimolecular quenching processes (Section 2), the efficiency of excited-state intermolecular proton transfer reactions depends on the lifetime of the excited state and the concentration of the reacting partner. Intramolecular photoinduced proton transfer processes (or ESIPT – excited-state intramolecular proton transfer), however, can be quite fast, and therefore represent efficient deactivation routes for excited states in (supra)molecular species containing both proton donors and acceptors.⁹

A different strategy to trigger acid–base reactions with light takes advantage of photoisomerization in compounds whose isomeric forms exhibit different acid–base properties. For example, the merocyanine species $11H^+$ shown in Fig. 14, upon irradiation at 400 nm in organic solution, is converted into the ring-closed spiropyran isomer **12** and releases a proton into the solution. In other words, compound $11H^+$ is a photoacid which generates H^+ ions upon irradiation with blue light and can protonate a basic species dissolved in the same solution. Compound $11H^+$ is slowly regenerated in the dark (on a time-scale of several hours in acetonitrile at room temperature), as a

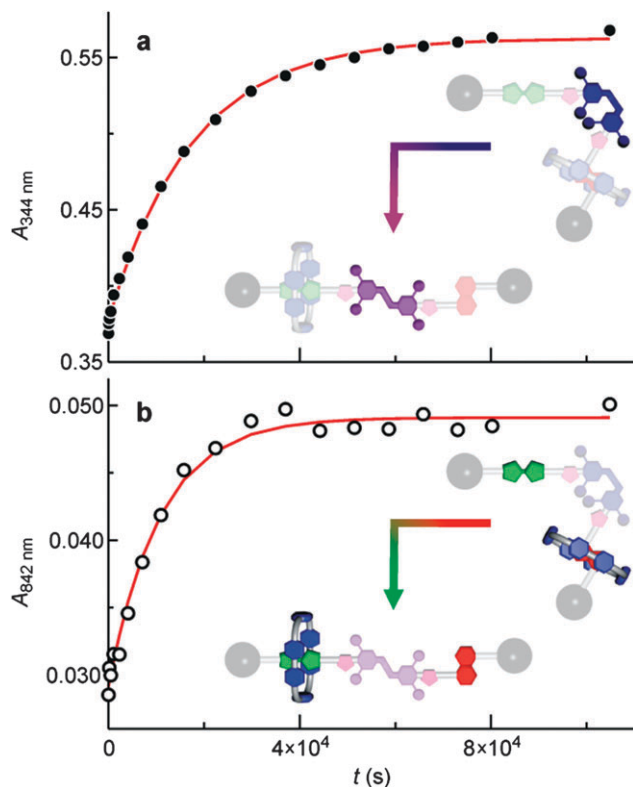


Fig. 13 Time-dependent absorption changes (CH_3CN , 295 K), monitored at (a) 344 nm, (*trans*-TMeAB absorption) and (b) 842 nm (macrocycle-TTF charge-transfer absorption), showing the regeneration of *trans*- 10^{4+} from the metastable state *cis*- 10^{4+} . The lines represent the data fitting according to a first-order kinetic equation. Adapted by permission from ref. 44.

consequence of the spontaneous ring opening of the spiroopyran isomer to yield a zwitterionic merocyanine form which takes the proton back (Fig. 14). Photoinduced proton transfer can thus be exploited to communicate a chemical signal from the photoacid to another acid–base sensitive molecular switch.^{45,46}

6.1 A molecular ensemble with luminescence properties controlled by photoinduced proton transfer

This concept was exploited to develop a solution-based chemical ensemble that employs a near-UV or blue light to control a photoluminescence output in the far-red spectral region.⁴⁷ The system can also be used to switch on/off the generation of singlet oxygen, which in turn exhibits phosphorescence in the near infrared. The ensemble (Fig. 14) consists of the above mentioned reversible photoacid 11H^+ and the acid–base sensitive complex $[\text{Os}(\text{pytpy})_2]^{2+}$ (pytpy = 4'-(pyridin-4-yl)-2,2':6',2''-terpyridine), 13^{2+} , in a 2 : 1 molar ratio.

Upon the addition of two equivalents of acid, 13^{2+} is converted into the 13H_2^{4+} species, protonated on the pendant pyridyl nitrogen atoms, which possesses different absorption and luminescence properties; specifically, while 13^{2+} has an emission band with $\lambda_{\text{max}} = 755$ nm (full line in Fig. 15a; $\Phi = 0.013$ and $\tau = 115$ ns in air equilibrated acetonitrile at room temperature), 13H_2^{4+} is very weakly emissive ($\lambda_{\text{max}} = 843$ nm, $\Phi \approx 4 \times 10^{-4}$, $\tau = 20$ ns). As the acid strength of the protonated

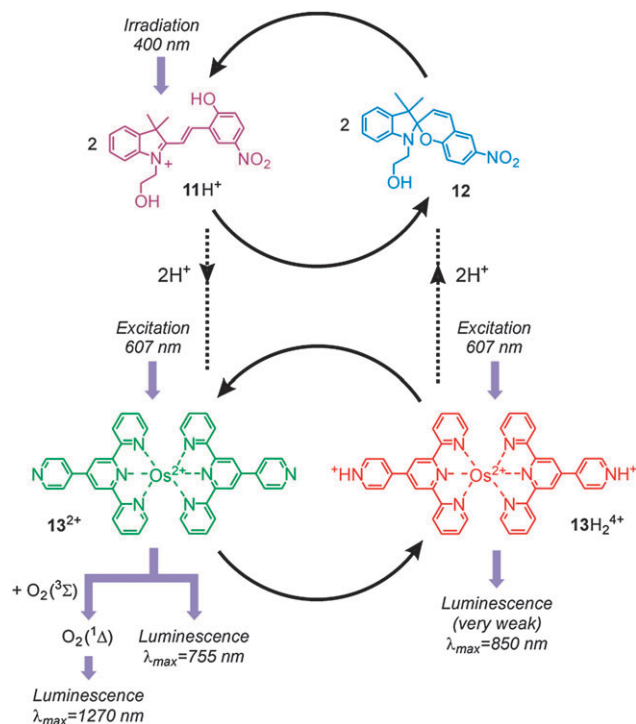


Fig. 14 Structural formulas and scheme of the coupled operation of the $11\text{H}^+/12$ photoacid system and the $13^{2+}/13\text{H}_2^{4+}$ switch in acetonitrile solution by means of photoinduced proton transfer.⁴⁷

pyridine is an intermediate of 11H^+ and 12 , it was envisaged that the protonation state of the osmium complex could be controlled by light using 11H^+ as a photoacid.

As schematized in Fig. 14, exhaustive irradiation of 11H^+ at 400 nm in acetonitrile causes the release of two equivalent protons which generate the 13H_2^{4+} species. This process can be monitored by (a) the disappearance of the absorption bands of 11H^+ and 13^{2+} , (b) the appearance of the absorption bands of 13H_2^{4+} , and (c) the quenching of the luminescence band of 13^{2+} at 755 nm (Fig. 15a, dashed line). Subsequent thermal equilibration in the dark regenerates the initial state by reverse proton exchange, as confirmed by the fact that the initial absorption and luminescence spectra are restored (Fig. 15a, dotted line). Several irradiation/thermal equilibration cycles can be repeated on the same solution without appreciable degradation of the components.

Another interesting feature of this system arises from the fact that the lifetime of the $^3\text{MLCT}$ excited state is substantially shortened on going from 13^{2+} to 13H_2^{4+} . Therefore, the chance that such an excited state becomes involved in bimolecular events (eqn (4)–(6)) is greatly diminished upon protonation of the metal complex. It follows that the photoinduced proton transfer between 11H^+ and 13^{2+} could be used to implement light control on the efficiency of bimolecular photosensitisation processes that originate from the osmium species. The feasibility of this idea can be demonstrated by relying on the fact that the $^3\text{MLCT}$ excited state of oligopyridine complexes of Os^{2+} is able to generate singlet oxygen ($^1\Delta$) with good efficiency by energy transfer to the triplet ground state ($^3\Sigma$) of O_2 .⁹ Hence, the formation of singlet oxygen (monitored by its characteristic

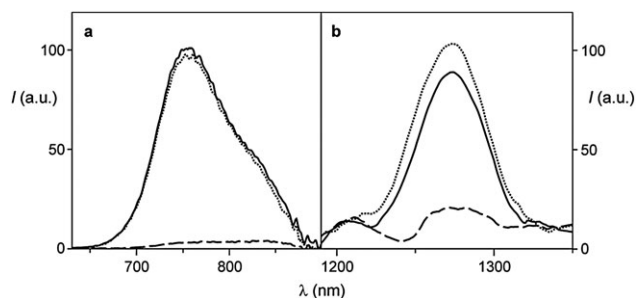


Fig. 15 Luminescence spectra ((a) far-red emission band of the osmium complex; (b) near infrared phosphorescence band of singlet oxygen) observed for an air equilibrated acetonitrile solution containing $18 \mu\text{M } \mathbf{11H}^+$ and $8.4 \mu\text{M } \mathbf{13}^{2+}$ (full lines), and of the same solution after exhaustive irradiation at 400 nm (dashed lines) and successive re-equilibration for 5 days at room temperature (dotted lines). In all cases excitation was performed at an isosbestic point at 607 nm.⁴⁷

phosphorescence at 1270 nm) in air equilibrated solutions upon excitation of the osmium species in the ³MLCT absorption band ($\lambda = 600\text{--}780 \text{ nm}$) was investigated for the ensemble of $\mathbf{11H}^+$ and $\mathbf{13}^{2+}$.⁴⁷

When a solution containing $18 \mu\text{M } \mathbf{7H}^+$ and $8.4 \mu\text{M } \mathbf{13}^{2+}$ is excited at 607 nm, the near infrared phosphorescence band of singlet oxygen is clearly observed (Fig. 15b, full line). Irradiation of the solution at 400 nm for 60 minutes generates the $\mathbf{12}$ and $\mathbf{13H}_2^{4+}$ species (Fig. 14); for this solution no emission peak in the near infrared is detected (Fig. 15, dashed line). Successive thermal re-equilibration of the solution regenerates $\mathbf{11H}^+$ and $\mathbf{13}^{2+}$, and the singlet oxygen phosphorescence can again be seen upon excitation of the metal complex (Fig. 15, dotted line). Interestingly, if the solution is irradiated at a wavelength at which both the photoacid and the metal complex absorb, a self-regulating behavior for singlet oxygen generation is observed.

This molecular switching ensemble exhibits a number of interesting features, namely: (i) it can process input and output optical signals in the visible region; (ii) at the same time, a near-UV light input can control a light output in the near infrared, thus bypassing the whole visible range; (iii) the outputs correspond to wavelengths in a spectral region (far red/near infrared) that is interesting, for instance, in communication technology and diagnostics; (iv) the photoluminescence output reading can be performed in a non-destructive manner; (v) a photochemical self-regulating behavior is observed under suitable conditions; (vi) owing to its reversibility and stability, the system can be cycled several times without appreciable loss of signal, and; (vii) the reset is thermally driven and thus does not imply the addition of chemicals and accumulation of byproducts. The main limitation of this system in view of real applications is the very slow thermal reset, which however could be exploited to obtain memory effects.^{45,46}

7. Conclusions and perspectives

The results reported in this review show that molecular devices and machines can be obtained by utilizing careful incremental design strategies, the tools of modern synthetic chemistry, and

the paradigms of supramolecular chemistry, together with some inspiration from natural systems. They also show that molecular devices and machines activated by photochemical energy inputs (through photoinduced energy- and electron-transfer processes) exhibit peculiar and interesting features: (i) these systems can work without formation of waste products; (ii) the amount of energy conferred to them by using photons can be precisely controlled by the wavelength and intensity of the exciting light, in relation to the absorption spectrum of the targeted species, (iii) such an energy can be transmitted without physically connecting them to the source (no “wiring” is necessary), the only requirement being the transparency of the matrix at the excitation wavelength; and (iv) in the particular case of molecular machines, they in general overcome energy barriers to operate by exploiting thermal fluctuations, the use of energy input as large as that provided by photoexcitation can lead the system to energy levels well above the barriers associated with mechanical motion in the electronic ground state; it is, therefore, possible that the mechanical movement corresponds to a downhill process with no appreciable activation barriers.

Another peculiar feature of photons is that they can also be useful to “read” that state of the system (by means of spectroscopic techniques), thereby monitoring its operation.

Concerning molecular devices, the examples illustrated in this review are mainly based on dendrimers that are characterized by unique structural aspects, such as a three dimensional array, generation-dependent size, the possibility to incorporate selected functional units at predetermined sites, and endo- and receptor capabilities. Because of these peculiarities, such compounds can not only play the role of light harvesting antennae and photoswitchable hosts, as outlined in the review, but can also be used as luminescent sensors with signal amplification, systems for energy up-conversion and for photocontrollable drug delivery. In future we expect that dendrimers will lead to even more exciting results in the fields of biology, medicine, and materials science, for example they constitute ideal scaffolds to deliver and release virus particles, to develop imaging compounds, diagnostic agents, new semiconductors and light emitting diodes.

The recent achievements on artificial molecular machines – some of which are illustrated here – enable interesting future developments to be devised, namely (i) the design and construction of more sophisticated systems showing complex motions and better performances in terms of stability, speed, switching, and so forth; (ii) the use of such systems to do molecular-level tasks such as uptake-release, transportation, catalysis, and mechanical gating of molecular channels; and (iii) the possibility of exploiting their logic behavior for information processing. In this regard, a chemical approach to molecular logic provides the opportunity to implement even complex logic operations with one molecule or supramolecular species. It is difficult, at the present stage, to predict which one of these two strategies will have the greater technological impact, if any. These and other questions regarding the advent of molecular computers (*e.g.*, serial or parallel architectures, solid-state or soft matter) represent one of the big challenges of nanotechnology.

The results described in this review also evidence that, although investigations of molecular devices and machines in solution are of fundamental importance, for some applications in the field of technology they have to be interfaced with the macroscopic world by ordering them in some way so that they can behave coherently and can be addressed in space. Viable possibilities include deposition on surfaces, incorporation into polymers, organization at interfaces, or immobilization onto membranes or porous materials. The recent achievements in this direction^{48–50} let one optimistically hope that useful materials and devices based on artificial molecular machines will see light in the not too distant future. To this aim, however, collaborative efforts from experts in different disciplines such as chemistry, physics, materials science and engineering – and possibly biology and medicine – are mandatory.

Although many problems related to the complex synthesis and operation of these systems, as well as issues concerning stability and reproducibility, remain to be solved, the research in this field shows that the potentialities of artificial molecular devices and machines are really huge and proves that at present we have discovered just the tip of the iceberg.

Acknowledgements

This work was supported by MIUR (PRIN 2010CX2TLM “InfoChem” and FIRB 2010RBAP11C58Y “Nanosolar”), ERC StG (PhotoSi, 278912) and the University of Bologna.

References

- 1 *Photobiology-The Science of Life and Light*, ed. L. O. Björn, Springer, New York, 2008.
- 2 J.-M. Lehn, *Angew. Chem., Int. Ed. Engl.*, 1988, **27**, 89.
- 3 V. Balzani, A. Credi and M. Venturi, *Chem.–Eur. J.*, 2002, **8**, 5524.
- 4 C. Joachim and J.-P. Launay, *Nouv. J. Chim.*, 1984, **8**, 723.
- 5 V. Balzani, L. Moggi and F. Scandola, in *Supramolecular Photochemistry*, ed. V. Balzani, Reidel, Dordrecht, 1987, p. 1.
- 6 V. Balzani, A. Credi and M. Venturi, *Molecular Devices and Machines – Concepts and Perspectives for the Nanoworld*, Wiley-VCH, Weinheim, 2008.
- 7 W. R. Browne and B. L. Feringa, *Nat. Nanotechnol.*, 2006, **1**, 25.
- 8 E. R. Kay, D. A. Leigh and F. Zerbetto, *Angew. Chem., Int. Ed.*, 2007, **46**, 72.
- 9 V. Balzani, P. Ceroni and A. Juris, *Photochemistry and Photophysics: Concepts, Research, Applications*, Wiley-VCH, in press.
- 10 See e.g.: G. Bergamini, E. Marchi and P. Ceroni, *Coord. Chem. Rev.*, 2011, **255**, 2458.
- 11 *Designing Dendrimers*, ed. S. Campagna, P. Ceroni and F. Puntoriero, Wiley, Hoboken, 2012.
- 12 A. M. Caminade, C. O. Turrin, R. Laurent, A. Ouali and B. Delavaux-Nicot, *Dendrimers: Towards Catalytic, Material and Biomedical Uses*, Wiley, Chichester, 2011.
- 13 V. Balzani, G. Bergamini, P. Ceroni and E. Marchi, *New J. Chem.*, 2011, **35**, 1944.
- 14 See e.g.: B. Branchi, P. Ceroni, V. Balzani, F.-G. Klärner and F. Vögtle, *Chem.–Eur. J.*, 2010, **16**, 6048.
- 15 M. E. Gallina, B. Baytekin, C. Schalley and P. Ceroni, *Chem.–Eur. J.*, 2012, **18**, 1528.
- 16 D. G. Kuroda, C. P. Singh, Z. Peng and V. D. Kleiman, *Science*, 2009, **326**, 263.
- 17 K. Toth, J. K. Molloy, M. Matta, B. Heinrich, D. Guillon, G. Bergamini, F. Zerbetto, B. Donnio, P. Ceroni and D. Felder-Flesch, *Angew. Chem., Int. Ed.*, 2013, **52**, 12303.
- 18 C. A. Parker and C. G. Hatchard, *Proc. Chem. Soc., London*, 1962, 386.
- 19 R. R. Islangulov, D. V. Kozlov and F. N. Castellano, *Chem. Commun.*, 2005, 3776.
- 20 T. N. Singh-Rachford and F. N. Castellano, *Coord. Chem. Rev.*, 2010, **254**, 2560.
- 21 P. Ceroni, *Chem.–Eur. J.*, 2011, **17**, 9560 and references therein.
- 22 G. Bergamini, P. Ceroni, P. Fabbrizi and S. Cicchi, *Chem. Commun.*, 2011, **47**, 12780.
- 23 D. Rehm and A. Weller, *Isr. J. Chem.*, 1970, **8**, 259.
- 24 *Electron Transfer in Chemistry*, ed. V. Balzani, Wiley-VCH, Weinheim, 2001, vol. 1–5.
- 25 V. Balzani, A. Credi and M. Venturi, *ChemSusChem*, 2008, **1**, 26, and references therein.
- 26 *Molecular Catenanes, Rotaxanes and Knots*, ed. J.-P. Sauvage and C. Dietrich-Buchecker, Wiley-VCH, Weinheim, 1999.
- 27 S. J. Loeb and J. A. Wisner, *Angew. Chem., Int. Ed.*, 1998, **37**, 2838.
- 28 G. J. E. Davidson, S. J. Loeb, P. Passaniti, S. Silvi and A. Credi, *Chem.–Eur. J.*, 2006, **12**, 3233.
- 29 E. C. Constable, C. E. Housecroft, A. Cargill Thompson, P. Passaniti, S. Silvi, M. Maestri and A. Credi, *Inorg. Chim. Acta*, 2007, **360**, 1102.
- 30 P. R. Ashton, R. Ballardini, V. Balzani, A. Credi, R. Dress, E. Ishow, C. J. Kleverlaan, O. Kocian, J. A. Preece, N. Spencer, J. F. Stoddart, M. Venturi and S. Wenger, *Chem.–Eur. J.*, 2000, **6**, 3558.
- 31 P.-L. Anelli, N. Spencer and J. F. Stoddart, *J. Am. Chem. Soc.*, 1991, **113**, 5131.
- 32 P. R. Ashton, R. Ballardini, V. Balzani, E. C. Constable, A. Credi, O. Kocian, S. J. Langford, J. A. Preece, L. Prodi, E. R. Schofield, N. Spencer, J. F. Stoddart and S. Wenger, *Chem.–Eur. J.*, 1998, **4**, 2413.
- 33 P. R. Ashton, V. Balzani, A. Credi, O. Kocian, D. Pasini, L. Prodi, N. Spencer, J. F. Stoddart, M. S. Tolley, M. Venturi, A. J. P. White and D. J. Williams, *Chem.–Eur. J.*, 1998, **4**, 590.
- 34 V. Balzani, M. Clemente-León, A. Credi, B. Ferrer, M. Venturi, A. H. Flood and J. F. Stoddart, *Proc. Natl. Acad. Sci. U. S. A.*, 2006, **103**, 1178.
- 35 A. Credi, M. Venturi and V. Balzani, *ChemPhysChem*, 2010, **11**, 3398.
- 36 P. Raiteri, G. Bussi, C. S. Cucinotta, A. Credi, J. F. Stoddart and M. Parrinello, *Angew. Chem., Int. Ed.*, 2008, **47**, 3536.
- 37 *Photochromism: Molecules and Systems*, ed. H. Dürr and H. Bouas-Laurent, Elsevier, Amsterdam, 2003.

- 38 H. M. D. Bandarab and S. C. Burdette, *Chem. Soc. Rev.*, 2012, **41**, 1809.
- 39 M. Baroncini, S. Silvi, M. Venturi and A. Credi, *Angew. Chem., Int. Ed.*, 2012, **51**, 4223.
- 40 H. A. Patel, S. Hyun Je, J. Park, D. P. Chen, Y. Jung, C. T. Yavuz and A. Coskun, *Nat. Commun.*, 2013, **4**, 1357.
- 41 S. Shinkai, T. Nakaji, T. Ogawa, K. Shigematsu and O. Manabe, *J. Am. Chem. Soc.*, 1981, **103**, 111.
- 42 T. Muraoka, K. Kinbara and T. Aida, *Nature*, 2006, **440**, 512.
- 43 E. Marchi, M. Baroncini, G. Bergamini, J. Van Heyst, F. Vögtle and P. Ceroni, *J. Am. Chem. Soc.*, 2012, **134**, 15277.
- 44 T. Avellini, H. Li, A. Coskun, G. Barin, A. Trabolsi, A. N. Basuray, S. K. Dey, A. Credi, S. Silvi, J. F. Stoddart and M. Venturi, *Angew. Chem., Int. Ed.*, 2012, **51**, 1611.
- 45 F. M. Raymo, *Adv. Mater.*, 2002, **14**, 401.
- 46 S. Silvi, E. C. Constable, C. E. Housecroft, J. E. Beves, E. L. Dunphy, M. Tomasulo, F. M. Raymo and A. Credi, *Chem.-Eur. J.*, 2009, **15**, 178.
- 47 S. Silvi, E. C. Constable, C. E. Housecroft, J. E. Beves, E. L. Dunphy, M. Tomasulo, F. M. Raymo and A. Credi, *Chem. Commun.*, 2009, 1484.
- 48 T. Kudernac, N. Ruangsapapichat, M. Parschau, B. Macia, N. Katsonis, S. R. Harutyunyan, K.-H. Ernst and B. L. Feringa, *Nature*, 2011, **479**, 208.
- 49 B. Lewandowski, G. De Bo, J. W. Ward, M. Papmeyer, S. Kuschel, M. J. Aldegunde, P. M. E. Gramlich, D. Heckmann, S. M. Goldup, D. M. D'Souza, A. E. Fernandes and D. A. Leigh, *Science*, 2013, **339**, 189.
- 50 S. F. M. van Dongen, J. Clerx, K. Nørsgaard, T. G. Bloemberg, J. J. L. M. Cornelissen, M. A. Trakselis, S. W. Nelson, S. J. Benkovic, A. E. Rowan and R. J. M. Nolte, *Nat. Chem.*, 2013, **5**, 945.